JB
Journals.ASM.org

Biochemical Characterization of the CDP-D-Arabinitol Biosynthetic Pathway in *Streptococcus pneumoniae* 17F

Quan Wang,[a,b,c] Yanli Xu,[a,b,c] Andrei V. Perepelov,[d] Yuriy A. Knirel,[d] Peter R. Reeves,[e] Alexander S. Shashkov,[d] Xi Guo,[a,b,c] Peng Ding,[a,b,c] and Lu Feng[a,f,g]

TEDA School of Biological Sciences and Biotechnology, Nankai University,[a] Key Laboratory of Molecular Microbiology and Technology, Ministry of Education,[b] and Engineering and Research Center for Microbial Functional Genomics and Detection Technology, Ministry of Education,[c] Tianjin, China; N. D. Zelinsky Institute of Organic Chemistry, Russian Academy of Sciences, Moscow, Russian Federation[d]; School of Molecular and Microbial Biosciences, University of Sydney, Sydney, NSW, Australia[e]; and Tianjin Key Laboratory of Microbial Functional Genomics[f] and Tianjin Research Center for Functional Genomics and Biochip,[g] Tianjin, China

***Streptococcus pneumoniae* is a major human pathogen associated with many diseases worldwide. Capsular polysaccharides (CPSs) are the major virulence factor. The biosynthetic pathway of D-arabinitol, which is present in the CPSs of several *S. pneumoniae* serotypes, has never been identified. In this study, the genes *abpA* (previously known as *abp1*) and *abpB* (previously known as *abp2*), which have previously been reported to be responsible for nucleoside diphosphate (NDP)-D-arabinitol (the nucleotide-activated form of D-arabinitol) synthesis, were cloned. The enzyme products were overexpressed, purified, and analyzed for their respective activities. Novel products produced by AbpA- and AbpB-catalyzing reactions were detected by capillary electrophoresis, and the structures of the products were elucidated using electrospray ionization mass spectrometry and nuclear magnetic resonance spectroscopy. As a result, *abpA* was identified to be a D-xylulose-5-phosphate cytidylyltransferase-encoding gene, responsible for the transfer of CTP to D-xylulose-5-phosphate (D-Xlu-5-P) to form CDP-D-xylulose, and *abpB* was characterized to be a CDP-D-xylulose reductase-encoding gene, responsible for the conversion of CDP-D-xylulose to CDP-D-arabinitol as the final product. The kinetic parameters of AbpA for the substrates D-Xlu-5-P and CTP and those of AbpB for the substrate CDP-D-xylulose and the cofactors NADH or NADPH were measured, and the effects of temperature, pH, and cations on the two enzymes were analyzed. This study confirmed the involvement of the genes *abpA* and *abpB* and their products in the biosynthetic pathway of CDP-D-arabinitol.**

Streptococcus pneumoniae is a major human pathogen associated with community-acquired pneumonia, septicemia, meningitis, and acute otitis media worldwide (3, 6). Capsular polysaccharides (CPSs) are the major virulence factor of *S. pneumoniae* (25). Ninety individual CPS serotypes have been recognized, and the CPS gene clusters responsible for the synthesis of all these serotypes, together with 54 CPS chemical structures, have been reported (4). Several kinds of sugars have been identified as components of these CPS structures, and genes for the synthesis of 14 nucleoside diphosphate (NDP) precursors of monosaccharides and alditols in the capsular gene clusters have been proposed. Of these, putative genes for NDP-D-arabinitol, NDP-D-mannitol, NDP-ribofuranose, and CDP-1-glycerol biosynthesis have been suggested, although biochemical activities have not yet been confirmed (1, 4).

To date, a number of biosynthetic pathways of rare sugars in *Escherichia coli* and *Shigella* have been characterized biochemically (22, 24), and these are useful for the pharmaceutical industry as a source of enzymes for the biotechnological production of some important monosaccharides. Recently, the biosynthetic pathway of CDP-2-glycerol in *S. pneumoniae* 23F was identified (23) by gene cloning, enzyme expression, and purification, followed by analysis of enzyme kinetic parameters and physical characterization of enzyme products using capillary electrophoresis (CE), mass spectrometry (MS), and nuclear magnetic resonance (NMR) spectroscopy.

D-Arabinitol is a five-carbon sugar alcohol and was found to occur in the CPS of *S. pneumoniae* 17F (9). The enzymes AbpA (previously known as Abp1) and AbpB (previously known as Abp2) have been proposed to be NTP-transferase and NAD-dependent epimerase/dehydratase, respectively, and involved in the synthesis of NDP-D-arabinitol, which is the nucleotide-activated form of D-arabinitol. In addition to *S. pneumoniae* 17F, AbpA and AbpB were also found to be present in the CPS gene clusters of *S. pneumoniae* 13, 24A, 24B, 24F, and 48, although there is now no CPS chemical structure information for these serotypes (4), which indicates that D-arabinitol is usually present in the CPS of *S. pneumoniae*. D-Arabinitol was also a characteristic major metabolite produced by several *Candida* species such as *Candida albicans* (5, 12) and was used as a biomarker for invasive candidiasis in human (19, 20, 26).

The biosynthetic pathway of NDP-D-arabinitol has been proposed to consist of a two-step process starting with D-xylulose-5-phosphate (D-Xlu-5-P) in *S. pneumoniae*. The precursor D-Xlu-5-P of this pathway is an intermediate of the pentose phosphate pathway and is converted from ribulose-5-phosphate by a ribulose-5-phosphate-3-epimerase (2). The exact nucleotide-activated form of D-arabinitol and its biosynthetic pathway have so far not been confirmed using molecular and biochemical techniques.

In this study, *abpA* and *abpB* from *S. pneumoniae* 17F were

Received 10 November 2011 **Accepted** 1 February 2012
Published ahead of print 10 February 2012
Address correspondence to Lu Feng, fenglu63@nankai.edu.cn.
Q.W. and Y.X. contributed equally to this article.
Supplemental material for this article may be found at http://jb.asm.org/.

doi:10.1128/JB.06487-11

TABLE 1 Bacterial strains, plasmids, and primers used in this study

Strain, plasmid, or primer	Description or sequence	Source[a]
Strains		
S. pneumoniae G1874	*S. pneumoniae* 17F type strain	CIDM
E. coli BL21(DE3)	F^- *ompT hsdS*$_B$(r_B^- m_B^-) *gal dcm* (DE3)	Novagen
E. coli DH5α	F^- f80*lacZ*ΔM15 *endA recA1 hsdR*(r_K^- m_K^-) *supE44 thi-1 gyrA96 relA1* (*lacZYA-argF*)*U169*	TBC
Plasmids		
pET28a$^+$	T7 express vector, Kan^r	Novagen
pET30a$^+$	T7 express vector, Kan^r	Novagen
pLW1212	pET28a$^+$ containing N-terminally six-histidine-tagged *S. pneumoniae* 17F *abpA* at the NdeI/BamHI site	This study
pLW1267	pET30$^+$ containing C-terminally six-histidine-tagged *S. pneumoniae* 17F *abpB* at the NdeI/BamHI site	This study
Primers		
wl-5894	5′-GGGAATTCCATATGATGAAAGTAGCGATTTTAACA-3′	
wl-5895	5′-CGCGGATCCCTATTTAATCCACTTATCTCGAG-3′	
wl-9063	5′-GGGAATTCCATATGATGACATTATTATTAAATAAAATATATAG-3′	
wl-9065	5′-CGCGGATCCGACTTTTCACTGGATAACTCCTT-3′	

[a] CIDM, Centre for Infectious Diseases and Microbiology, Westmead Hospital, New South Wales, Australia; TBC, Tianjin Biochip Corporation, Tianjin, China.

cloned and the gene products were expressed and purified. By CE, MS, and NMR analysis of AbpA- and AbpB-catalyzing reaction products and substrate specificity analysis of AbpA, the two enzymes AbpA and AbpB were identified as D-xylulose-5-phosphate cytidylyltransferase and CDP-D-xylulose reductase, respectively, thus confirming that CDP-D-arabinitol is the nucleotide-activated form of D-arabinitol and providing biochemical confirmation of the CDP-D-arabinitol biosynthetic pathway. The kinetic and physicochemical parameters of these enzymes were also characterized.

MATERIALS AND METHODS

Bacterial strains and plasmids. The bacterial strains and plasmids used in this study are listed in Table 1.

Cloning and plasmid construction. The *abpA* and *abpB* genes from *S. pneumoniae* 17F (G1874) were amplified by PCR using the primers listed in Table 1 (wl-5894 and wl-5895 for *abpA*, wl-9063 and wl-9065 for *abpB*). A total of 30 cycles were performed using the following conditions: denaturation at 95°C for 30 s, annealing at 50°C for 30 s, and extension at 72°C for 1 min (final volume, 20 μl). The amplified genes, *abpA* and *abpB*, were cloned into pET28a$^+$ and pET30a$^+$, respectively, to construct pLW1212 (containing *abpA*) and pLW1267 (containing *abpB*). The presence of the inserts was confirmed by sequencing using an ABI 3730 sequencer.

Protein expression and purification. *Escherichia coli* BL21 carrying each of pET28a$^+$, pET30a$^+$, and the recombinant plasmids was cultured in LB medium containing 50 μg/ml kanamycin overnight at 37°C. The overnight culture (4 ml) was inoculated into 200 ml of fresh LB medium and cultured at 37°C until the A_{600} reached 0.6. Expression of AbpA and AbpB was induced with 0.1 mM isopropyl-β-D-thiogalactopyranoside (IPTG) for 4 h at 25°C. Subsequently, cells were harvested by centrifugation, washed with binding buffer (50 mM Tris-HCl, pH 7.4, 300 mM NaCl, 10 mM imidazole), and resuspended in 5 ml of the same buffer containing 1 mM phenylmethylsulfonyl fluoride (PMSF) and 1 mg/ml of lysozyme. Samples were sonicated, cell debris was removed by centrifugation, and total soluble proteins in the supernatant were collected. The His_6-tagged fusion proteins in the supernatant were purified by nickel ion affinity chromatography with a chelating Sepharose fast-flow column (GE Healthcare), according to instructions provided by the manufacturer. Unbound proteins were removed with 100 ml wash buffer (50 mM Tris-HCl, pH 7.4, 300 mM NaCl, and 25 mM imidazole). Fusion proteins were eluted in 3 ml elution buffer (50 mM Tris-HCl, pH 7.4, 300 mM NaCl, and 250 mM imidazole) and dialyzed for at least 4 h against 50 mM Tris-HCl buffer (pH 7.4) at 4°C. Protein concentration was determined by the Bradford method.

Molecular masses of AbpA and AbpB. The molecular masses of His_6-tagged AbpA and AbpB were analyzed by a 4700 Proteomics analyzer (ABI). Sample aliquots of 0.3 μl were mixed with 0.3 μl acid α-cyano-4-hydroxycinnamic acid (CHCA) solution and then spotted on the plate. The mass spectrometer was operated under a 18-kV accelerating voltage in the reflectron mode with an *m/z* range of 20,000 to 50,000. Peak lists (signal-to-noise ratio [*S/N*] > 10) obtained from matrix-assisted laser desorption ionization–time of flight MS were extracted from the raw data.

Enzyme activity assays. The assay for AbpA activity was carried out in a final volume of 20 μl containing 50 mM Tris-HCl buffer (pH 7.4), 10 mM $MgCl_2$, 5 mM D-Xlu-5-P (Sigma-Aldrich), 2.5 mM CTP, 2.5 mU inorganic pyrophosphatase (Sigma-Aldrich), and 0.018 mM purified AbpA at 37°C for 0.5 h. The assay for AbpB activity was carried out at 37°C for 1 h in a final volume of 20 μl containing the 5 μl of the finished AbpA reaction mixture (containing 0.625 mM CDP-D-xylulose) plus 0.625 mM NADPH and 7.58 μM AbpB. Products of the reactions were analyzed by CE and electrospray ionization (ESI) MS. Enzyme activities were indicated by the conversion of substrates into products.

Determination of temperature, optimal pH, and divalent cation requirements. For characterization of the parameters required for optimal enzymatic activity, 5.62 μM AbpA and 0.38 μM AbpB were used and the reactions were carried out at 37°C for 30 min (AbpA) or 40 min (AbpB). To determine the optimum temperature for AbpA and AbpB activity, reactions were carried out at 4, 15, 25, 37, 50, 55, 60, 65, and 75°C. To determine the optimum pH for AbpA activity, reactions were carried out at pH 4.5, 5, 5.5, 6, 6.5, 7, 7.4, 8, and 8.5. To analyze the effects of different cations on AbpA activity, reactions were carried out in the presence of 10 mM KCl, NH_4Cl, $NiSO_4$, $MgCl_2$, $MnCl_2$, $FeSO_4$, $CuCl_2$, $CaCl_2$, $CoCl_2$, $ZnCl_2$, and $FeCl_3$. Enzyme activity was determined by CE.

Kinetic parameter measurements. To measure the AbpA K_m and maximum rate of metabolism (V_{max}) values, reactions were carried out with 0.094 μM AbpA in a final volume of 20 μl at various concentrations of D-Xlu-5-P (0.2 to 2 mM) and a constant concentration of CTP (2.5 mM) or at various concentrations of CTP (0.3 to 3 mM) or dCTP (0.5 to 6 mM) and a constant concentration of D-Xlu-5-P (10 mM), and the other constituents were the same as those described for the enzyme activity assays. To measure the AbpB K_m and V_{max} values, reactions were carried out with 0.19 μM AbpB (for CDP-D-xylulose and NADH) or 0.095 μM AbpB (for NADPH) in a final volume of 20 μl at various concentrations of CDP-D-xylulose (0.25 to 2 mM) and a constant concentration of NADH (0.625 mM) or at various concentrations of NADH (0.2 to 4 mM) or

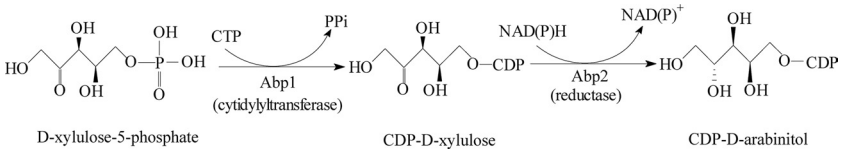

FIG 1 Biosynthetic pathway of CDP-D-arabinitol.

NADPH (0.2 to 4 mM) and a constant concentration of CDP-D-xylulose (0.625 mM). The reactions were carried out using the enzymes with a single preparation, which was preserved with 20% glycerol at −80°C. The reactions were terminated by adding an equal volume of chloroform. Conversion of D-Xlu-5-P and CTP to CDP-D-xylulose, CDP-D-xylulose to CDP-D-arabinitol, and NADH to NAD^+ or NADPH to $NADP^+$ was monitored by CE. K_m and V_{max} values were calculated on the basis of the Michaelis-Menten equation. The reported data are the averages of results from three independent experiments.

CE analysis. CE was performed using a Beckman Coulter P/ACE MDQ capillary electrophoresis system with a photodiode array (PDA) detector (Beckman Coulter, CA). The capillary was bare silica (75 μm [internal diameter] by 57 cm), and the detector was set at 50 cm. The capillary was conditioned before each run by washing with 0.1 M NaOH for 2 min, deionized water for 2 min, and 25 mM borate-NaOH (pH 9.6) (used as the mobile phase) for 2 min. Samples were loaded by pressure injection at 0.5 lb/in^2 for 10 s, and separation was carried out at 20 kV. Peak integration and trace alignment were obtained using a Beckman P/ACE station software (32 Karat, version 5.0). The conversion ratio was calculated by comparing the peak areas of substrate and product.

RP HPLC and ESI MS analysis. The AbpA and AbpB reaction mixtures were separated by reversed-phase high-performance liquid chromatography (RP HPLC) using an LC-20AT HPLC (Shimadzu, Japan) with a Venusil MP-C_{18} column (5-μm particle size, 4.6 by 250 mm; Agela Technologies, Inc.). The mobile phase was composed of 5% acetonitrile and 95% 50 mM triethylamine-acetic acid (pH 6.48), applied at a flow rate of 0.6 ml/min. Fractions containing the expected products were collected, lyophilized, and redissolved in water before being injected into a Finnigan LCQ Advantage MAX ion trap mass spectrometer (Thermo Fisher, CA) in negative mode (4.5 kV, 250°C) for ESI MS analysis. For MS/MS (MS2) analysis, nitrogen and helium were used as the collision and auxiliary gases, respectively, with typical collision energies of 20 eV to 30 eV.

Sugar analysis. A sample of the AbpB product was dephosphorylated with aqueous 48% hydrofluoric acid (0.2 ml, 4°C, 20 h). The product was acetylated with a 1:1 (vol/vol) mixture of pyridine and acetic anhydride (100°C, 1 h) and analyzed by gas-liquid chromatography (GLC) using an Agilent 7820 chromatograph equipped with an HP-5 column (0.32 mm by 30 m) and a temperature program of 160 (1 min) to 290°C at 7°C min^{-1}.

NMR spectroscopy. Samples were deuterium exchanged by freeze-drying from 99.5% D_2O, dissolved in 99.95% D_2O (150 μl), and examined using a Shigemi (Japan) microtube at 25°C. NMR spectra were recorded on a Bruker Avance II 600 spectrometer (Germany) using internal sodium 3-trimethylsilylpropanoate-2,2.3.3-d_4 (chemical shift for H [δ_H], 0), external acetone (δ_C, 31.45), and external aqueous 85% H_3PO_4 (δ_P, 0) as calibration references. Two-dimensional NMR spectra were obtained using standard Bruker software, and the Bruker TopSpin (version 2.1) program was used to acquire and process the NMR data. A mixing time of 100 ms was used in a total correlation spectroscopy (TOCSY) experiment.

RESULTS

Overexpression and purification of enzymes. Plasmids pLW1212 (containing *abpA*) and pLW1267 (containing *abpB*) were constructed, and the expression of AbpA and AbpB was induced in transformed *Escherichia coli* BL21 by IPTG. The majority of the proteins were observed in the soluble fraction by SDS-PAGE analysis (data not shown), and the proteins were purified to near homogeneity as His_6-tagged fusion proteins by nickel ion affinity chromatography (see Fig. S1 in the supplemental material). The molecular masses of His_6-tagged AbpA (29 kDa) and AbpB (40 kDa) estimated by SDS-PAGE analysis corresponded well with the calculated molecular masses (29.0 and 41.4 kDa, respectively).

The molecular masses of His_6-tagged AbpA and AbpB were also analyzed by 4700 Proteomics analyzer (see Fig. S2 in the supplemental material). For AbpA, the mass peak (*m/z* 28,941.37) was in agreement with the calculated molecular mass of 28,986.58 Da. For AbpB, the mass peak (*m/z* 41,433.75) corresponded with the calculated molecular mass of 41,428.38 Da. Another mass peak of AbpB (*m/z* 42,424.90) was also found, and it was proposed to be AbpB combined with NADPH (molecular weight [MW], 833.4) or NADH (MW, 709.4).

Characterization of AbpA and AbpB activities by CE. The proposed biosynthetic pathway of CDP-D-arabinitol involving AbpA and AbpB is illustrated in Fig. 1. The pathway was characterized by carrying out each of the enzymatic steps sequentially in a single reaction mixture containing D-Xlu-5-P as the initial substrate and comparing the reaction products with standard compounds using CE (Fig. 2). A new peak that eluted at 13.4 min was identified from the catalysis of CTP by AbpA (Fig. 2A). This peak was converted to another new peak that eluted at 12.9 min on the addition of AbpB and NADPH/NADH to the AbpA-catalyzed reaction mixture, and NADPH/NADH was converted to $NADP^+$/NAD^+ (Fig. 2B and C). No products were obtained when heat-denatured AbpA and AbpB were used in the reaction mixture or when purified proteins from *E. coli* BL21 carrying the plasmids pET28a$^+$ and pET30a$^+$ were used instead of AbpA and AbpB in the reaction mixture.

Identification of AbpA and AbpB products by ESI MS and tandem MS. Products of the AbpA and AbpB reactions were purified by RP HPLC. Fractions containing the AbpA and AbpB products were collected and analyzed by negative-mode ESI MS (see Fig. S3 in the supplemental material). Ion peaks were obtained at *m/z* 534.10 (see Fig. S3A in the supplemental material) and 536.18 (see Fig. S3C in the supplemental material), which were consistent with the expected masses for CDP-D-xylulose (535.29 Da) and CDP-D-arabinitol (537.30 Da). MS2 analysis of the two ion peaks revealed that the ion peaks matched the fragments derived from CDP-D-xylulose and CDP-D-arabinitol (see Fig. S3B and D in the supplemental material, respectively), which are depicted in Table 2.

Chemical analysis of the AbpB product. The AbpB product was dephosphorylated with 48% hydrofluoric acid, and the resultant pentitol was acetylated. GLC analysis showed a peak of pentitol acetate with a retention time identical to that of the authentic arabinitol acetate (see Fig. S4 in the supplemental material) and different from the retention times of ribitol ace-

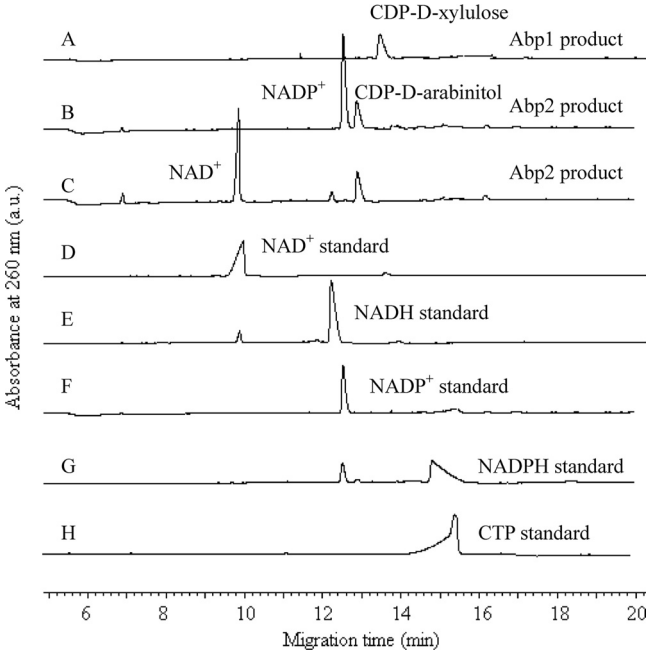

FIG 2 CE chromatography of AbpA and AbpB products. (A) AbpA reaction products (0.25 mM); (B) AbpB reaction products (0.25 mM) with NADPH as cofactor; (C) AbpB reaction products (0.25 mM) with NADH as cofactor; (D) NAD^+ standard (1 mM); (E) NADH standard (1 mM); (F) $NADP^+$ standard (0.2 mM); (G) NADPH standard (0.5 mM); (H) CTP standard (0.4 mM). a.u., absorbance units.

tate and xylitol acetate. This finding demonstrated that the pentitol derived from the AbpB product has the *arabino* configuration.

Determination of structure of AbpB product using NMR spectroscopy. A sample of the AbpB product was studied by ^1H, ^{13}C, and ^{31}P NMR spectroscopy, including two-dimensional ^1H,^1H correlation spectroscopy and TOCSY, H-detected ^1H,^{13}C heteronuclear single quantum coherence (HSQC), and H-detected ^1H,^{31}P heteronuclear multiple-quantum correlation (HMQC) experiments. In the TOCSY spectrum, cross-peaks were observed between all protons within each spin system, including those between H-1′ and H-2′–H-5a′,b′ of ribofuranose; H-1a,1b and H-2 of arabinitol; H-5a,b and H-3,H-4 of arabinitol; and H-5 and H-6 of cytosine. The ^{13}C NMR signals for the ribose and arabinitol moieties were assigned using a two-dimensional ^1H,^{13}C HSQC experiment. The assigned chemical shifts (δ) of ribose (Table 3) were in accordance with published data for ribose-5-phosphate (10, 23). A comparison of the data for the arabinitol moiety in the AbpB product and free D-arabinitol (Table 3) showed downfield displacements due to phosphorylation of the H-1a,1b and C-1 signals from d 3.67,3.69 and 64.3 to d 4.02,4.04 and 68.2, respectively. Lower downfield displacements were also observed for H-2 and H-3 and upfield displacements were observed for C-2 and C-3, whereas the positions of the signals for H-4, H-5a,5b, C-4, and C-5 were virtually unchanged (Table 3). The ^{31}P NMR spectrum contained signals for a diphosphate group at d −10.7 and −11.1, which, as expected, showed strong correlations with H-5a′,5b′ of ribose at d −11.1/4.21,4.28 and H-1a,1b of arabinitol at d −10.7/4.02, 4.04 in the ^1H,^{31}P HMQC spectrum. These data demonstrated that the AbpB product is CDP-D-arabinitol (Fig. 3).

Determination of physicochemical parameters: optimal temperature and pH for AbpA and AbpB activities. Activities of AbpA and AbpB at temperatures ranging from 4 to 75°C are shown in Fig. 4a. For AbpA, the activity showed the highest conversion ratio (84.7%) at 37°C. For AbpB, the conversion ratio was highest (67.2%) at 25°C and greatly decreased at 65°C and above. AbpA had a broad pH range of activities, with an optimum pH of between 6.0 and 9.0 and with the highest conversion ratio being 74.0% at pH 7.4 (Fig. 4b).

Effects of divalent cations on the activity of AbpA. The effects of cations, including K^+, NH_4^+, Mg^{2+}, Ca^{2+}, Cu^{2+}, Co^{2+}, Fe^{3+}, Mn^{2+}, Ni^{2+}, Zn^{2+}, and Fe^{2+}, on the activity of AbpA are shown in Fig. 4c. Compared to reactions with no cations, it was noted that AbpA activity increased in the presence of Mg^{2+}, Fe^{2+}, Co^{2+}, Fe^{3+}, Mn^{2+}, Ni^{2+}, and Zn^{2+}. Mg^{2+} and Fe^{2+} were favorable for the reaction, with conversion ratios of 84.2 and 84.0%, respectively. AbpA activity in the presence of Co^{2+}, Fe^{3+}, Mn^{2+}, Ni^{2+}, and Zn^{2+} was lower, with conversion ratios ranging from 55.3 to 78.3%. Cu^{2+} partially inhibited AbpA activity, and NH_4^+, K^+, and Ca^{2+} had no obvious effects on AbpA activity. Decreased AbpA activity was detected in the presence of the cation-chelating agent EDTA.

Kinetic parameters of AbpA and AbpB activity. Kinetic parameters of AbpA for two substrates (D-Xlu-5-P and CTP) and of AbpB for one substrate (CDP-D-xylulose) and two cofactors (NADH or NADPH) were measured. Initial velocities were measured and used for the kinetic parameter calculations. The kinetics of the reaction catalyzed by AbpA and AbpB fit to the Michaelis-Menten model (see Fig. S5 in the supplemental material). The K_m values of AbpB are 1.88 mM for NADH and 1.14 mM for NADPH, and AbpB has a higher k_{cat}/K_m ratio for NADPH (2,154.47 $mM^{-1} \cdot min^{-1}$) than for NADH (98.91 $mM^{-1} \cdot min^{-1}$), indicating a preference for NADPH as the cofactor.

TABLE 2 Interpretations of ion peaks presented in ESI MS and MS2

Composition of fragment	Molecular formula	Mol wt	Mass (negative)
CDP-D-xylulose (full scan)			
CDP-D-xylulose-Na	$C_{14}H_{22}O_{15}N_3P_2Na$	557.27	556.09
CDP-D-xylulose	$C_{14}H_{23}O_{15}N_3P_2$	535.29	534.10
CDP-D-xylulose (MS2-534.10)			
CDP + H_2O	$C_9H_{16}N_3O_{12}P_2$	420.18	419.93
CDP-D-xylulose minus CH_2(OH)$COCH_2OH$	$C_{11}H_{18}O_{12}N_3P_2$	446.22	444.11
CDP − PO_3	$C_9H_{14}N_3O_8P$	323.19	322.00
D-Xylulose-PO_3	$C_5H_9O_7P$	212.09	210.88
D-Xylulose-PO_3-PO_3	$C_5H_{10}O_{10}P_2$	292.07	290.76
CDP-D-arabinitol (full scan)			
CDP-D-arabinitol-Na	$C_{14}H_{24}O_{15}N_3P_2Na$	559.28	558.08
CDP-D-arabinitol	$C_{14}H_{25}O_{15}N_3P_2$	537.30	536.18
CDP-D-arabinitol (MS2-536.18)			
CDP − H_2O	$C_9H_{12}N_3O_{10}P_2$	384.15	383.96
D-Arabinitol-PO_3-PO_2	$C_5H_{14}O_9P_2$	280.10	279.15
CDP − PO_3	$C_9H_{14}N_3O_8P$	323.19	322.00
D-Arabinitol-PO_3	$C_5H_{11}O_7P$	214.11	212.56

TABLE 3 ^{1}H and ^{13}C NMR data for CDP-D-arabinitol and D-arabinitol as model compounds

Moiety	Nucleus	δ (ppm) at the following atoms:						
		1a,1b	2	3	4	5a,5b	5	6
D-Arabinitol	^{1}H	3.67,3.69	3.93	3.58	3.76	3.66,3.84		
	^{13}C	64.3	71.5	71.7	72.2	64.2		
CDP-D-arabinitol								
Arabinitol	^{1}H	4.02,4.04	4.09	3.66	3.76	3.66,3.84		
	^{13}C	68.2	70.0	71.1	72.1	64.2		
β-Ribofuranose[a]	^{1}H	6.01	4.33	4.36	4.28	4.21,4.28		
	^{13}C	90.3	75.5	70.4	83.9	65.8		
Cytosine	^{1}H						6.14	7.98
	^{13}C						97.8	Not determined

[a] Data for β-ribofuranose are for the 1′, 2′, 3′, 4′, and 5a′,5b′ atoms instead of the 1, 2, 3, 4, and 5a,5b atoms, respectively.

The detailed kinetic parameters for the two enzymes are listed in Table 4.

Substrate specificity for AbpA. Four substrates, including those for AbpA (D-Xlu-5-P) and other cytidylyltransferases (D-glucose-1-phosphate [13, 21], glycerol-2-phosphate [23], and fructose-6-phosphate [our unpublished study]), were used for analysis of the AbpA substrate specificity. AbpA activity was detected only in the presence of D-Xlu-5-P and not in the presence of other sugar phosphates (data not shown). Among the nucleotide phosphate donors tested (CTP, dCTP, ATP, dATP, ADP, dGTP, dTTP) for AbpA-catalyzed reactions, only CTP and dCTP were identified as active donors, with average conversion ratios of 100% and 62%, respectively (see Fig. S6 in the supplemental material). Furthermore, the k_{cat}/K_m ratio for CTP (660.55 $mM^{-1} \cdot min^{-1}$) was higher than that for dCTP (499.58 $mM^{-1} \cdot min^{-1}$), indicating that CTP is the preferred NTP donor in this reaction.

DISCUSSION

D-Arabinitol is found or proposed to be present in the CPSs of many *S. pneumoniae* serotypes, and it was also found to be a major metabolite product of *Candida albicans* (5, 12). Therefore, D-arabinitol may play an important role in the virulence of pathogens, including *S. pneumoniae* and *C. albicans*.

This study provided full characterization of the biosynthetic pathway of CDP-D-arabinitol in *S. pneumoniae*. The pathway was shown to occur via a two-step process starting with D-Xlu-5-P and catalyzed by AbpA (D-xylulose-5-phosphate cytidylyltransferase) and AbpB (CDP-D-xylulose reductase). The *rpe* gene has been biochemically identified to encode a ribulose-5-

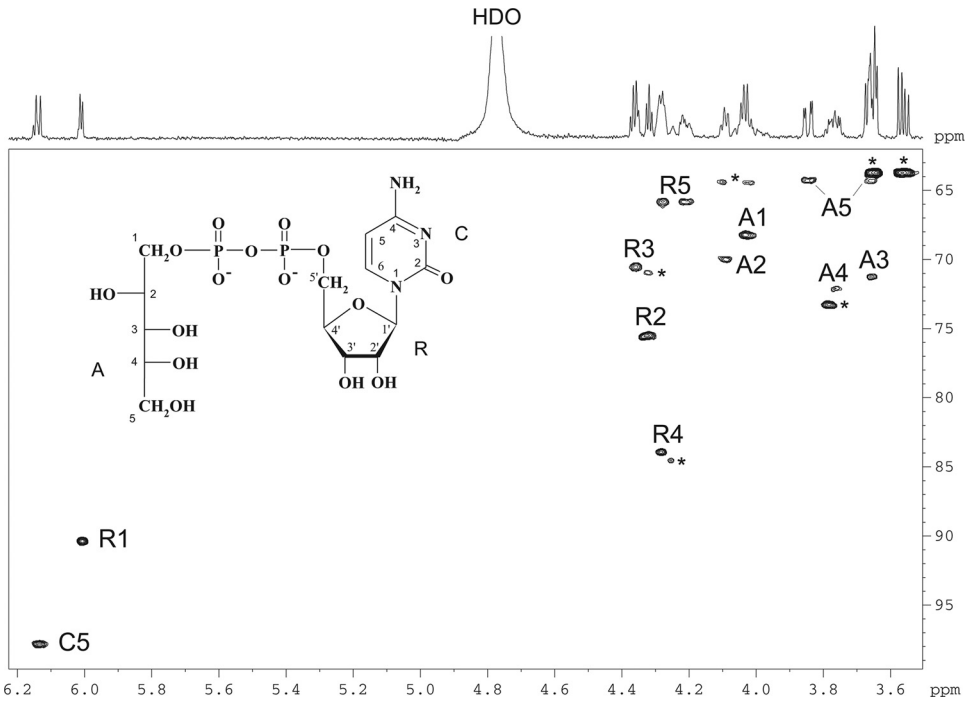

FIG 3 Part of a two-dimensional $^{1}H,^{13}C$ HSQC spectrum of CDP-D-arabinitol. The corresponding part of the ^{1}H NMR spectrum is displayed along the horizontal axis. Arabic numerals refer to cross-peaks in the ribose, arabinitol, and cytosine moieties, designated R, A, and C, respectively. Signals of CMP and glycerol contaminants are marked with an asterisk. The structure of CDP-D-arabinitol is shown in the inset. HDO, hydrogen deuterium oxide.

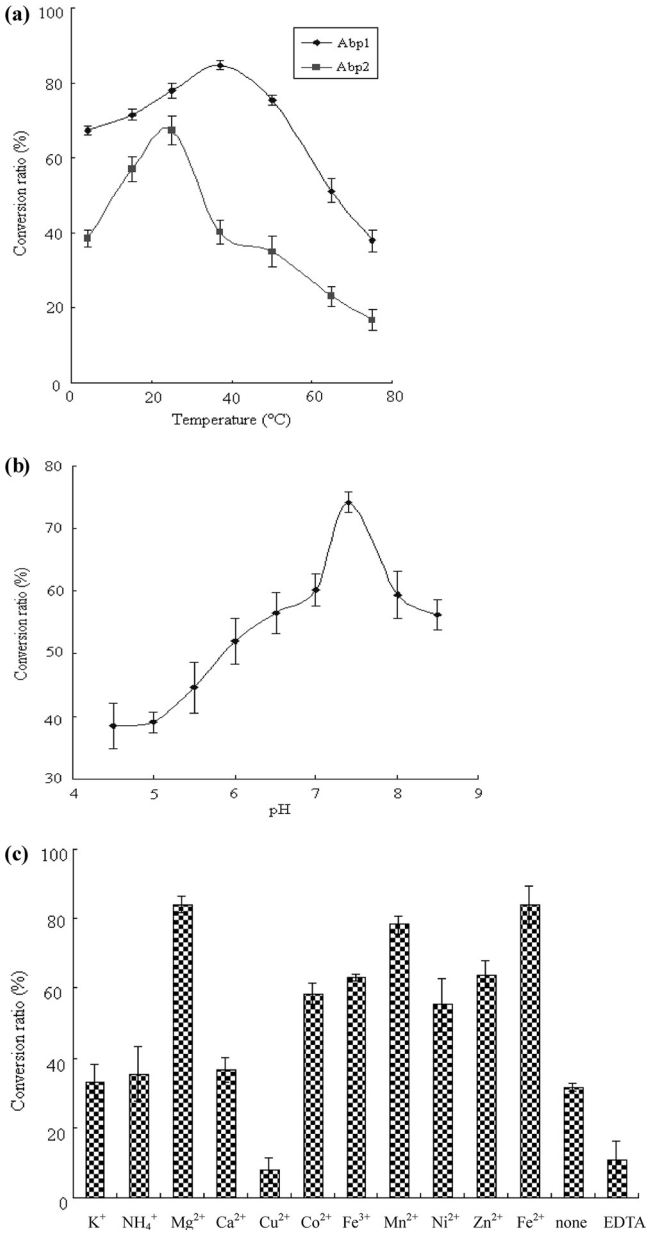

FIG 4 Effects of temperature (a) on the conversion ratios of AbpA and AbpB and the effects of pH (b) and cations (c) on the conversion ratio of AbpA.

phosphate-3-epimerase that catalyzes the conversion of ribulose-5-phosphate to D-Xlu-5-P in the pentose phosphate pathway (2, 7), and this gene is present on the *S. pneumoniae* chromosome.

AbpA shares 34% to 53% identity with 2-*C*-methyl-D-erythritol-4-phosphate cytidylyltransferase (IspD) from several bacterial species, such as *Parabacteroides distasonis*, *Prevotella bryantii*, and *Enterococcus faecalis*, and all these proteins were found to belong to the same protein family (UPF0007) by searching the Pfam library. Comparisons of AbpA and 2-*C*-methyl-D-erythritol-4-phosphate cytidylyltransferases from different species revealed that all the proteins contained two conserved motifs: AXGXGXR X_6PK and (V/I)X(I/H)HDXXR (see Fig. S7 in the supplemental material). The first motif is very similar to a previously reported motif, AAGXGXRX_5PK, in IspD proteins, which, coupled with Gly 82, Asp 83, and Ser 88, is involved in sequestering CTP and methyl-CDP (18). The corresponding Gly and Ser are also present in AbpA and all of the 2-*C*-methyl-D-erythritol-4-phosphate cytidylyltransferases (see Fig. S7 in the supplemental material). The second motif is similar to a characteristic signature motif of IspD, (V/I)L(V/I)HDXAR. Most of the key residues responsible for binding and processing of substrates, including Arg 20, Lys 27, Arg 157, Lys 215, Arg 109, and Asp 106 (16, 18) were also identified in AbpA (see Fig. S7 in the supplemental material). Maximal AbpA activity occurred in the presence of Mg^{2+}. This phenomenon has also been reported for other IspD proteins (18) and therefore suggests that the catalytic mechanism of AbpA is similar to that of IspD.

AbpA activity was shown to be inhibited in the presence of Cu^{2+}, and Cu^{2+} has been found to inhibit the activities of many enzymes (22, 23). As it was reported that Cu^{2+} could combine with enzyme molecules or the enzyme-substrate complexes (15), the possible explanation for the inhibition of Cu^{2+} is that the combination of Cu^{2+} with AbpA or AbpA-substrate decreases the enzyme activity.

AbpB shares 35% to 46% identity with epimerase/dehydratases from many species and belongs to the NAD-dependent epimerase/dehydratase family (PF01370), which contains proteins that use nucleotide-sugars as the substrates and NAD(P)H as a cofactor. NADPH was identified as a cofactor for AbpB activity in this study. Alignments of AbpB and other NAD-dependent epimerase/dehydratases identified two motifs, GXXGXXG and SX_{30}YXXXK, in AbpB (see Fig. S8 in the supplemental material). The motif GXXGXXG, located near the N terminus of the proteins, is similar to the motif (GXGXXA, GXG XXG) involved in the binding of cofactor NAD(P)H (8, 17). The second motif is very similar to the previously reported motif SX_{24} YXXXK in a dehydrogenase from *Comamonas testosteroni*, in which the Ser, Tyr, and Lys residues play important roles in catalytic activity (11, 14).

Rare sugars are potentially useful in the pharmaceutical industry. However, chemical synthesis of such sugars is complicated by the requirement for multistep reactions of protection and depro-

TABLE 4 Kinetic parameters

Enzyme	Substrate	K_m (mM)	V_{max} (mM min^{-1})	k_{cat} (min^{-1})	k_{cat}/K_m ($mM^{-1} \cdot min^{-1}$)
AbpA	D-Xylulose-5-phosphate	1.02 ± 0.08	0.16 ± 0.003	1,638.0 ± 306.5	1,639.9 ± 422.6
AbpA	CTP	1.76 ± 0.14	0.10 ± 0.005	1,065.3 ± 60.9	610.5 ± 84.6
AbpA	dCTP	2.85 ± 0.08	0.15 ± 0.01	1,602.6 ± 106.8	563.8 ± 53.3
AbpB	CDP-D-xylulose	1.53 ± 0.09	0.09 ± 0.01	486.8 ± 76.3	322.2 ± 68.8
AbpB	NADH	1.88 ± 0.17	0.035 ± 0.015	190.0 ± 81.2	101.5 ± 49.8
AbpB	NADPH	1.14 ± 0.11	0.23 ± 0.038	2,456.1 ± 396.9	2,192.1 ± 512.5

tection. Therefore, the enzymes AbpA and AbpB characterized in this study represent valuable resources for the biotechnological production of CDP-D-arabinitol.

ACKNOWLEDGMENTS

This study was supported by grants from the National Basic Research Program of China (973 Program) (2012CB721001, 2012CB721101, 2011CB504900), the National Natural Science Foundation of China (NSFC) Key Program (31030002), the Chinese National Science Fund for Distinguished Young Scholars (30788001) and General Program (30900255, 81071392, 30870070, 31111120026), the Tianjin Research Program of Application Foundation and Advanced Technology (10JCYBJC10100), the Fundamental Research Funds for the Central Universities (65020121, 65020061), and the Russian Foundation for Basic Research (11-04-91173-NNSF and 11-04-01020).

REFERENCES

1. **Aanensen DM, Mavroidi A, Bentley SD, Reeves PR, Spratt BG.** 2007. Predicted functions and linkage specificities of the products of the *Streptococcus pneumoniae* capsular biosynthetic loci. J. Bacteriol. **189**:7856–7876.
2. **Akana J, et al.** 2006. D-Ribulose 5-phosphate 3-epimerase: functional and structural relationships to members of the ribulose-phosphate binding (beta/alpha)8-barrel superfamily. Biochemistry **45**:2493–2503.
3. **Austrian R.** 1999. The pneumococcus at the millennium: not down, not out. J. Infect. Dis. **179**(Suppl 2):S338–S341.
4. **Bentley SD, et al.** 2006. Genetic analysis of the capsular biosynthetic locus from all 90 pneumococcal serotypes. PLoS Genet. **2**:e31.
5. **Bernard EM, Christiansen KJ, Tsang SF, Kiehn TE, Armstrong D.** 1981. Rate of arabinitol production by pathogenic yeast species. J. Clin. Microbiol. **14**:189–194.
6. **Cartwright K.** 2002. Pneumococcal disease in Western Europe: burden of disease, antibiotic resistance and management. Eur. J. Pediatr. **161**:188–195.
7. **Chen YR, Larimer FW, Serpersu EH, Hartman FC.** 1999. Identification of a catalytic aspartyl residue of D-ribulose 5-phosphate 3-epimerase by site-directed mutagenesis. J. Biol. Chem. **274**:2132–2136.
8. **Jiang F, Hellman U, Sroga GE, Bergman B, Mannervik B.** 1995. Cloning, sequencing, and regulation of the glutathione reductase gene from the cyanobacterium *Anabaena* PCC 7120. J. Biol. Chem. **270**:22882–22889.
9. **Jones C, Aguilera B, van Boom JH, Buchanan JG.** 2002. Confirmation of the D configuration of the 2-substituted arabinitol 1-phosphate residue in the capsular polysaccharide from *Streptococcus pneumoniae* type 17F. Carbohydr. Res. **337**:2353–2358.
10. **Jones C, Whitley C, Lemercinier X.** 2000. Full assignment of the proton and carbon NMR spectra and revised structure for the capsular polysaccharide from *Streptococcus pneumoniae* type 17F. Carbohydr. Res. **325**:192–201.
11. **Jornvall H, et al.** 1995. Short-chain dehydrogenases/reductases (SDR). Biochemistry **34**:6003–6013.
12. **Kiehn TE, Bernard EM, Gold JW, Armstrong D.** 1979. Candidiasis: detection by gas-liquid chromatography of D-arabinitol, a fungal metabolite, in human serum. Science **206**:577–580.
13. **Lindqvist L, Kaiser R, Reeves PR, Lindberg AA.** 1994. Purification, characterization, and high performance liquid chromatography assay of *Salmonella* glucose-1-phosphate cytidylyltransferase from the cloned *rfbF* gene. J. Biol. Chem. **269**:122–126.
14. **Oppermann U, et al.** 2003. Short-chain dehydrogenases/reductases (SDR): the 2002 update. Chem. Biol. Interact. 143–144:247–253.
15. **Palmer T.** 1995. Understanding enzymes, 4th ed. Prentice Hall/Ellis Horwood, New York, NY.
16. **Richard SB, et al.** 2004. Kinetic analysis of *Escherichia coli* 2-C-methyl-D-erythritol-4-phosphate cytidyltransferase, wild type and mutants, reveals roles of active site amino acids. Biochemistry **43**:12189–12197.
17. **Scrutton NS, Berry A, Perham RN.** 1990. Redesign of the coenzyme specificity of a dehydrogenase by protein engineering. Nature **343**:38–43.
18. **Shi W, et al.** 2007. Biosynthesis of isoprenoids: characterization of a functionally active recombinant 2-C-methyl-D-erythritol 4-phosphate cytidyltransferase (IspD) from *Mycobacterium tuberculosis* H37Rv. J. Biochem. Mol. Biol. **40**:911–920.
19. **Stradomska TJ, et al.** 2005. Urinary D-arabinitol/L-arabinitol levels in infants undergoing long-term antibiotic therapy. J. Clin. Microbiol. **43**:5351–5354.
20. **Stradomska TJ, et al.** 2010. Determination of urinary D-/L-arabinitol ratios as a biomarker for invasive candidiasis in children with cardiac diseases. J. Med. Microbiol. **59**:1490–1496.
21. **Thorson JS, Kelly TM, Liu HW.** 1994. Cloning, sequencing, and overexpression in *Escherichia coli* of the alpha-D-glucose-1-phosphate cytidylyltransferase gene isolated from *Yersinia pseudotuberculosis.* J. Bacteriol. **176**:1840–1849.
22. **Wang Q, et al.** 2008. Characterization of the dTDP-D-fucofuranose biosynthetic pathway in *Escherichia coli* O52. Mol. Microbiol. **70**:1358–1367.
23. **Wang Q, et al.** 2010. Characterization of the CDP-2-glycerol biosynthetic pathway in *Streptococcus pneumoniae.* J. Bacteriol. **192**:5506–5514.
24. **Wang Y, et al.** 2007. Biochemical characterization of dTDP-D-Qui4N and dTDP-D-Qui4NAc biosynthetic pathways in *Shigella dysenteriae* type 7 and *Escherichia coli* O7. J. Bacteriol. **189**:8626–8635.
25. **Watson DA, Musher DM, Verhoef J.** 1995. Pneumococcal virulence factors and host immune responses to them. Eur. J. Clin. Microbiol. Infect. Dis. **14**:479–490.
26. **Yeo SF, Zhang Y, Schafer D, Campbell S, Wong B.** 2000. A rapid, automated enzymatic fluorometric assay for determination of D-arabinitol in serum. J. Clin. Microbiol. **38**:1439–1443.